ACTA METALLURGICA SLOVACA
2021, VOL. 27, NO. 4, 180-184

RESEARCH PAPER

THE EFFECT OF EGGSHELL AS A REINFORCEMENT ON THE MECHANICAL AND CORROSION PROPERTIES OF MG-ZN-MN MATRIX COMPOSITE

H.A. El-Fattah [1,3], M. K. Gouda [1], Salah Salman [1,2], Ayman Elsayed [4]*

[1] Department of Mining and Petroleum Engineering, Faculty of Engineering, Al-Azhar University, Nasr City, Cairo, 11371, Egypt
[2] Institute of Innovation for Future Society, Nagoya University, 464-8603, Nagoya, Japan.
[3] Alexandria Higher Institute of Engineering and Technology (AIET), Alexandria, 21311, Egypt.
[4] Powder Technology Department., Central Metallurgical Research and Development Institute, Cairo, Egypt

*Corresponding author: mohammedgouda@azhar.edu.eg, Faculty of Engineering, Al-Azhar University, Nasr City, Cairo, 11371, Egypt

Received: 05.08.2021
Accepted: 06.10.2021

ABSTRACT

Magnesium is a promising lightweight metal required in many industries such as automobile, aerospace, electronics, etc. It is also a biodegradable material, which eliminates the secondary removal procedure of the implant. Furthermore, its mechanical properties are similar to the mechanical properties of human bone. In this research, eggshells were used as an environmentally friendly composite reinforcement material in the Mg-2.5Zn-1Mn matrix. Composites were prepared using the powder metallurgy route. The effect of eggshells on the morphology, mechanical, and corrosion behaviour of Mg-2.5Zn-1Mn alloy was investigated. The results revealed an enhancement in grain refining ability and mechanical properties of Mg-2.5Zn-1Mn with eggshell additives. The corrosion behaviour improved at a higher percentage of eggshells (10%)

Keywords: Magnesium, Composite materials, Eggshells, Corrosion.

INTRODUCTION

Magnesium (Mg) is the third-largest structural metal in the earth's crust; it comes after aluminum and iron. Mg and Mg-alloys attribute high strength to weight ratio. For example, typical magnesium alloys weigh less than their aluminum coequal counterparts with the same stiffness [1-3]. These properties cause magnesium alloys to be a good candidate for lightweight applications like aerospace and transportation [4].
Generally, Mg ions are readily available in the human body and have a role in various metabolic activities and biological functions. Moreover, Mg can be dissolved, consumed, or absorbed gradually, reflecting its high biocompatibility and biodegradability [5, 6]. Furthermore, the typical stress shielding effect reported in some other commonly used metallic implants can be avoided in Mg alloys as their elastic modulus and compressive yield strength of magnesium are closer to those of natural bone [7-10].
Mg is usually alloyed with alloying elements like aluminum (Al), zinc (Zn), silicon (Si), zirconium (Zr), manganese (Mn), and rare earth elements (e.g., Ce, Nd, Gd, etc.) [11]. Most of these alloying elements have low biocompatibility, particularly Al and rare earth elements. Thus, it is crucial to develop fully biocompatible Mg-based material with appropriate strength for biomedical applications [12-14].
From the point of view of biocompatibility, element selection should be limited to the nutrient elements in the human body such as Ca, Mn, Zn, and Sn [15-17]. Zn is considered the primary alloying element with Mg because of its biocompatibility and favorable impact upon strength. Nevertheless, the Zn content should be limited to 4 wt.% to achieve the desired mechanical properties [18].
Recently, many researchers turned in the direction toward alloying Mg with biodegradable alloying elements such as Zn and Ca. For example, Wan et al. found that a magnesium alloy containing 0.6 wt.% calcium content have good corrosion and mechanical properties and could be used as a new biomedical alloy [2]. Moreover, Ikeo et al. concluded that extrusion at various temperatures for Mg–0.5 wt% Ca alloy led to solid solution hardening and grain refinement resulting in high strength comparable to titanium alloys [19].
Nevertheless, the disadvantages of Mg, like low strength and subcutaneous gas bubbles caused by rapid corrosion [6, 20] limits its use as a biomedical material. Therefore, most of the researchers are trying to overcome these common problems. Alloying and grain refinement are the most widely used strategies to enhance strength and corrosion resistance. However, using non-biocompatible elements limits the applicability of Mg in the biomedical field [21-25].
As a result, the advantages of employing metal matrix composites (MMCs) over monolithic metals, such as greater specific modulus and higher specific strength, allow for the use of this type of engineering material in various applications and industries. Therefore, these advantages open the door for using this class of engineering material in various applications and industries. Furthermore, because of their low density and high specific strength, magnesium MMCs can be used in structural components in aerospace and biomedical applications [26].
In the meantime, the need for sustainable low-cost materials is rising. Many researchers are hardly trying to use renewable low-cost reinforcements like fly ash, red mud, and Kankara clay (aluminosilicate) [27, 28]. Therefore, in the present study, an environmentally friendly composite material using the

eggshells as a reinforcement in the Mg-2.5Zn-1Mn matrix was prepared using the powder metallurgy route. The effect of eggshells on the morphology, mechanical, and corrosion behaviour of Mg-2.5Zn-1Mn alloy is investigated.

MATERIAL AND METHODS

The Mg composite has been prepared by using the powder metallurgy technique. Elemental powders of pure Mg, Zn, and Mn of 99.5 % purity and 50 to 100 microns particle size, along with eggshell powders, were used. The eggshell powder was prepared by collecting the waste of used chicken eggshell. All organic matter was removed, washed, and dried at 100 °C in a muffle furnace for about 10 minutes. After drying, eggshell bulk samples were grinded to a size range of 150–200 μm using a hammer mill.

The Mg-composites of Mg-2.5%Zn-1%Mn reinforced with eggshell with 0, 1, 5, and 10% concentrations were prepared by ball milling in PQ-N2 4-jar planetary ball mill (Across International Inc.). All element concentrations are stated as weight percentages. The mechanical alloying process was performed for 2 hours under an argon gas atmosphere in a 0.5-litre stainless steel jar using 300 rpm and the ball to powder ratio of 10:1.

Consolidation of the composites has been obtained by using cold compaction and hot isostatic pressing. Cold compaction was first performed on rectangular cross-section steel die using the pressure of 600 MPa. Then the compacted billets were consolidated by the hot isostatic press (HP-630 American Isostatic Press Inc.) at 550 ˚C and 210 MPa argon gas pressure. The temperature was increased from room temperature to 550 ˚C at the rate of 5 ˚C/min. Simultaneously, the pressure was increased to its maximum value, followed by holding for 1 hr.

Composite characterization has been done using metallurgical tests as well as hardness. Firstly, the actual densities of the obtained composites were calculated using Archimedes' principle. Samples were precision weighed in an electronic balance to an accuracy of 0.01 g. Porosity levels of the composite materials were calculated using the following equation:

$$\% \text{ porosity} = \frac{(\rho_{Theortical} - \rho_{Actual})}{(\rho_{Theortical} - \rho_{air})} \times 100 \quad (1.)$$

The optical microstructure was obtained using an optical microscope (Olympus, ID No. 3609) after sample grinding with emery papers and polishing with a diamond paste of 0.3 microns particle size. Scanning electron microscopy and energy-dispersive x-ray spectroscopy were obtained using (JEM-6500F, JEOL) and (XRD-6100, Shimadzu) testers. Micro-hardness tests (HMV-G Micro Vickers Hardness Tester, Shimadzu) were conducted on samples after surface polishing using the load of 100 g for 10 sec, and an average of 15 hardness readings was reported.

Finally, the corrosion properties were investigated through potentiodynamic curves using a typical three-electrode cell configuration with Ag/AgCl electrode as reference electrode and platinum wire as a counter electrode in addition to the studied sample with 1 cm surface area as a working electrode. The electrolyte was the physiological Ringer's solution at 37 °C, and each run was performed after 30 min immersion in open-circuit potential condition. The scan rate was 5 mV s-1 using (Princeton Eg&G model) potentiostat.

RESULTS AND DISCUSSION

Density and compositional homogeneity

The composites in the current study were fabricated by powder metallurgy technique. It is considered the optimum choice for producing such MMCs mainly because of the high production rates combined with the good compositional homogeneity. Moreover, powder metallurgy is economically beneficial when compared to other techniques [29].

Table 1 lists the density results of the obtained samples. Rule of mixtures (ROM) was used to calculate the theoretical densities. The actual measured density of the obtained composites was less than the theoretical densities as expected. Moreover, the higher density of eggshells (2.17 g /cm^3) increases the density from 1.93037 to 1.96157 gm/cm^3 at an ES concentration of 10%. Therefore, the porosity percentage is also increased by increasing the ES content. However, these porosity levels are still within the allowed limits, which means that the powder metallurgy technique in the current study can obtain near-dense materials. However, increased porosities (>1%) at higher weight percentages of ES (5 and 7%) may be due to the higher degree of agglomeration of ES particles in Mg matrix. [12].

Table 1 Density and porosity values of the obtained composites

Sample name	ρ Theoretical (g/cm^3)	ρ Actual (g/cm^3)	Relative density	Porosity (%)
Mg-2.5Zn-1Mn	1.93037	1.8864	97.724	2.276
Mg-2.5Zn-1Mn-1ES	1.93349	1.8796	97.213	2.787
Mg-2.5Zn-1Mn-5ES	1.94597	1.8676	95.973	4.027
Mg-2.5Zn-1Mn-10ES	1.96157	1.8669	95.176	4.824

The compositional homogeneity was checked through microstructure investigation combined with EDS analysis. **Fig. 1** shows the EDS mapping of the Mg-2.5Zn-1Mn-10ES composite. As shown in this figure, Mg is uniformly distributed, ES particle is clear in the middle with an irregular shape, Mn and Zn fine particles are scattered. Moreover, the results show that there is no transformation from eggshell particles to any secondary precipitate. Also, eggshell particles appear with irregular shapes due to the effect of ball milling. This shape is favorable to elude stress concentration sites during mechanical loading.

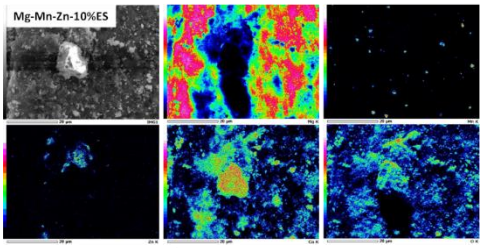

Fig. 1 EDS mapping of Mg-2.5Zn-1Mn-10ES composite

Microstructure and phases

The microstructure images of the studied composites are shown in **Fig. 2**. In this figure, composites showed a combination between equiaxed grains with some amounts of elongated grains, particularly at higher amounts of eggshells, as shown in Fig. 2 d. It is known that the equiaxed nature of grains significantly impacts strength and corrosion behaviour [30]. Moreover, a slight grain size reduction is noted by comparing the images from (a) to (d); in other words, the increasing ES percentages led to a slight grain refining of ES composites.

This is probably because of the pining effect of hard ES particles along the grain boundaries of the obtained composite, thereby inhibiting the grain growth process, as shown in Fig. 2 and Fig. 3. Moreover, the eggshell particles with sub-micron size, which may enclose the eggshell particles in the ball-milled powder, may create sub-micron dense zones affecting the process of grain size refinement. Because of the dynamic recrystallization of the grains, which leads to grain refinement, micron-submicron-sized particles have been found to be advantageous to trigger particle-assisted nucleation [31].
Gupta et al. [32] and Parande et al. [30] previously reported that the addition of ES causes a considerable grain refinement in Mg-Zn alloy with an agreement with the behaviour observed in the current study. Furthermore, images of microstructures reveal that eggshell particles prefer to segregate along grain boundaries, as indicated with arrows in **Fig. 2**. The segregation seems to increase with increasing of the ES percentage since in the lower ES compositions it is quite limited, while it is significant at higher ES composition as shown in Fig. 2. Therefore, it is expected that segregation along grain boundaries limited the expected further grain refining reported in previous reports [30, 32].

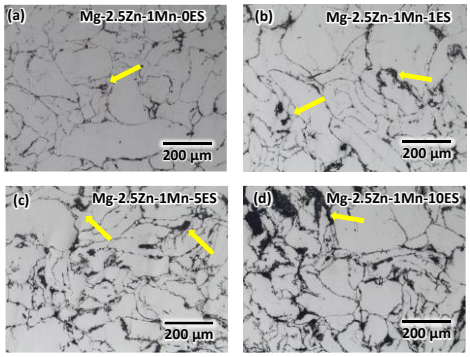

Fig. 2 Microstructure of the obtained composite (compositions are indicated at each image)

Fig. 3 shows the scanning electron microscope images for ES composites. As can be noticed from this figure, the eggshell particles are nearly uniformly dispersed in the Mg– n–Mn matrix. Moreover, the amount of ES particles has increased with the increase of the ES percentages from 1 to 10%. Furthermore, the grain refining increasing with increasing of ES amount in the composite

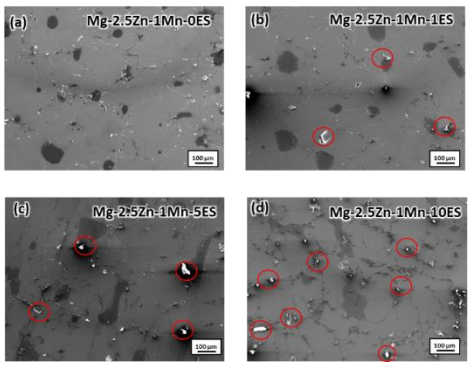

Fig. 3 SEM images of the obtained composite (compositions are indicated at each image)

The X-ray diffraction generated peaks of all composites are shown in **Fig. 4**. In this figure, high-intensity peaks related to Mg were identified in all obtained composites. Nevertheless, low-intensity peaks associated to $CaCO_3$ were detected only at composite contains higher than 5% ES. This mostly because of the low volume fraction of ES in the matrix at compositions lower than 5% ES. Moreover, this is also the reason for undetected peaks corresponding to other secondary phases. One of the limitations of XRD technique is that phases related peaks are undetectable if the volume fraction is ≤ 2.5 vol.% in the matrix [33, 34]. Furthermore, no peaks for intermetallic compounds and no distinct peak shifts imply that the lowest interfacial interaction occurs throughout the production process [30].

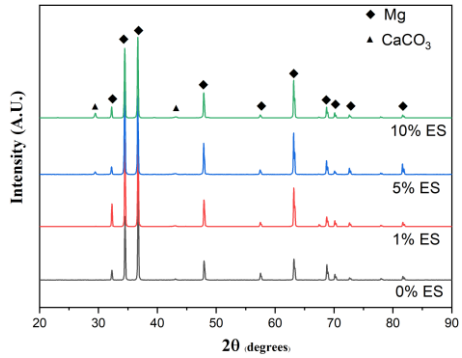

Fig. 4 XRD patterns of the obtained compositions

Mechanical properties
Microhardness (Hv) values of the developed composites are listed in **Table 2**. As can be noticed in this table, the addition of 1% ES increases the value of microhardness by approximately 7 %. However, further increasing the amount of ES resulted in a slight increase in microhardness values. The improvement in the microhardness values is mainly because of the distribution of hard ES particulate inside the matrix [35, 36]. Moreover, the dispersion strengthening of metallic materials reported in the literature [11] results in this increase in the microhardness values.

Table 2 Hardness readings statistics of Mg-2.5%Zn-1%Mn-ES

Samples	ES composition			
	0%	*1%*	*5%*	*10%*
Maximum	55.5	55.3	65.2	62.9
Minimum	32.3	40.2	34.1	32.9
Average	46.0	49.0	50.1	51.0
Standard deviation	6.9	3.9	7.6	7.6

Corrosion behavior
The corrosion behaviours of ES composites were investigated using potentiodynamic polarization curve measurements, as shown in **Fig. 5**. The electrolyte was the physiological Ringer's solution at 37 °C, and each run was performed after 30 min immersion in open-circuit potential condition. The values of corrosion current density (I_{corr}) and corrosion potential (E_{corr}), which extracted from the Tafel plot, were used to characterize the corrosion behaviour and calculation of corrosion rate in (mm y^{-1}).
The corrosion rate can be calculated using Faraday's law in terms of penetration rates as per ASTM G102-89 [37]:

$$\text{Corrosion rate (mm.y}^{-1}) = K \times I_{corr} \times \frac{EW}{\rho} \quad (2.)$$

Where K is the corrosion constant (K = 0.00327 if the corrosion rate is mm/yr.), Icorr is the corrosion current density (μA/cm2), EW is an equivalent weight; ρ is density (g/cm^3) of the alloy.

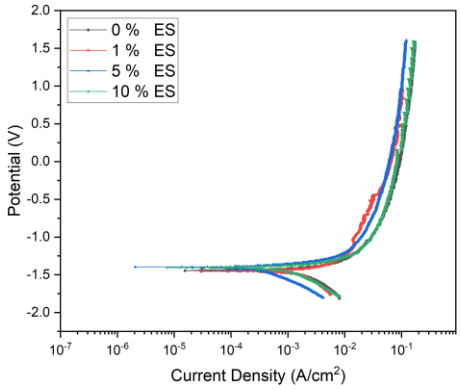

Fig. 5 shows the effect of ES on the Potentiodynamic polarization curves of Mg-2.5%Zn-1%Mn-xES composites

To calculate the alloy's equivalent weight, the following approach may be used. Consider a unit mass of alloy is oxidized. The electron equivalent for 1 g of an alloy, Q, is then:

$$\sum nifi/wi \quad (3.)$$

where: *fi* is the mass fraction of the i $^{th.}$ element in the alloy.
Wi is the atomic weight of the i $^{th.}$ element in the alloy, and
ni is the valence of the i$^{th.}$ element of the alloy.
Therefore, the alloy equivalent weight, EW, is the reciprocal of this quantity:

$$EW = \frac{1}{Q} \quad (4.)$$

The corrosion results were summarized in **Table 3**. The addition of 1wt. % of ES has a negative effect on the corrosion resistance of ES composites. However, by increasing the ES concentration to 5%, a slight improvement in the anticorrosion behaviour was observed. Further increase in the ES concentration to 10% results in a decrease in anticorrosion behaviour.

Table 3 Corrosion essential parameters of Mg-2.5%Zn-1%Mn-xES composites

	ES composition			
	0%	*1%*	*5%*	*10%*
E_{corr}, Vvs. Ag/AgCl	-1.4	-1.5	-1.37	-1.39
I_{corr}uA.cm^{-2} vs. Ag/AgCl	1.4	3.9	1.2	3.1
Corrosion rate mm.y^{-1}	0.0282	0.0784	0.0234	0.0614

5% ES composite has the highest Ecorr, the lowest Icorr, and the lowest corrosion rate, as shown in **Table 2**. This means that the corrosion properties of the Mg-2.5Zn-1Mn matrix are fluctuating by increasing the ES concentration. Therefore, 5wt.% addition of ES can be considered the most suitable composite in the current study. This decrease in corrosion resistance was probably related to the formation of micro galvanic cells between the matrix elements and the reinforcement. Moreover, it was reported that Mg_2Ca phases precipitated along grain boundaries with increasing Ca content lead to a deterioration of the mechanical properties and corrosion resistance of Mg alloys [38]. Mg_2Ca phase was not detectable by XRD, possibly due to its small volume fraction. However, it is still probably one of the reasons for this deterioration in the anticorrosion properties.
The current results agree with Bakhsheshi-Rad et al. [39] when investigating Mg-Ca alloys in-vitro corrosion behaviour with varying Ca content. They found that the corrosion rate of Mg-Ca alloys increased significantly with higher amounts of Ca. These results are significant and promising to use this ES composite as a biodegradable material. However, further improvement in the corrosion resistance is still required.

CONCLUSION

In this study, near-dense composite materials from eggshells, magnesium, zinc, and manganese were prepared using powder metallurgy technique. Eggshells were successfully used as an environmentally friendly reinforcement material in the Mg-2.5Zn-1Mn matrix. Mg and $CaCO_3$ were the only existing phases at higher eggshells concentrations (10 wt. %). The addition of eggshells increases the microhardness by 7%. The corrosion properties improved by adding eggshells up to 5%; however, further increase in the concentration of eggshells results in a decrease in the corrosion properties. Mg-2.5Zn-1Mn-5ES is a potential biomedical composite material that could be considered for further investigation.

REFERENCES

1. G. J. Simandl, H. Schultes, J. Simandl, S. Paradis: *Magnesium-Raw Materials, Metal Extraction and Economics-Global Picture*. The Ninth Biennial SGA Meeting, Dublin, Irish Association of Economic Geology, 2007, 827-831.
2. Y. Wan, G. Xiong, H. Luo, F. He, Y. Huang X. Zhou: Materials & Design, 29(10), 2008, 2034-2037. https://doi.org/10.1016/j.matdes.2008.04.017.
3. G. L. Makar, J. Kruger: International Materials Reviews, 38(3), 1993, 138-153. https://doi.org/10.1179/imr.1993.38.3.138.
4. G. L. Song, A. Atrens: Advanced Engineering Materials, 1(1), 1999, 11-33. https://doi.org/10.1002/(SICI)1527-2648(199909)1:1<11::AID-ADEM11>3.0.CO;2-N.
5. M. P. Staiger, A. M. Pietak, J. Huadmai G. Dias, Biomaterials, 27(9), 2006, 1728-1734. https://doi.org/10.1016/j.biomaterials.2005.10.003.
6. G. Song, S. Song: Advanced Engineering Materials, 9(4), 2007, 298-302. https://doi.org/10.1002/adem.200600252.
7. N. Li, Y. Zheng: Journal of Materials Science & Technology, 29(6), 2013, 489-502. https://doi.org/10.1016/j.jmst.2013.02.005.
8. E. Zhang, L. Xu, K. Yang: Scripta Materialia, 53(5), 2005, 523-527. https://doi.org/10.1016/j.scriptamat.2005.05.009.
9. M. I. Jamesh, G. Wu, Y. Zhao, D. R. McKenzie, M. M. M. Bilek, P. K. Chu: Corrosion Science, 91, 2015, 160-184. https://doi.org/10.1016/j.corsci.2014.11.015.
10. A. Atrens, M. Liu, N. I. Zainal Abidin: Materials Science and Engineering: B, 176(20), 2011, 1609-1636. https://doi.org/10.1016/j.mseb.2010.12.017.
11. M. Gupta, N. M. L. Sharon: Magnesium Alloys. In: *Magnesium, Magnesium Alloys, and Magnesium Composites*. Hoboken, New Jersey, USA, John Wiley & Sons, Inc., 2011, p. 39-85. https://doi.org/10.1002/9780470905098.ch3.
12. H. Hermawan: Biodegradable Metals: State of the Art. In: *Biodegradable Metals: From Concept to Applications.* Berlin,

Heidelberg, Springer Berlin Heidelberg, 2012, p. 13-22. https://doi.org/10.1007/978-3-642-31170-3_2.
13. R. J. Narayan: Philosophical Transactions of the Royal Society A, 368(1917), 2010, 1831-1837. https://doi.org/10.1098/rsta.2010.0001.
14. L. L. Hench, J. M. Polak: Science, 295(5557), 2002, 1014-1017. https://doi.org/10.1126/science.1067404.
15. X. Gu, Y. Zheng, Y. Cheng, S. Zhong, T. Xi: Biomaterials, 30(4), 2009, 484-498. https://doi.org/10.1016/j.biomaterials.2008.10.021.
16. Y. J. Chen, Y. J. Li, J. C. Walmsley, S. Dumoulin, P. C. Skaret, H. J. Roven: Materials Science and Engineering: A, 527(3), 2010, 789-796. https://doi.org/10.1016/j.msea.2009.09.005.
17. Y. Nakamura, Y. Tsumura, Y. Tonogai, T. Shibata, Y. Ito: Toxicological Sciences, 37(2), 1997, 106-116. https://doi.org/10.1093/toxsci/37.2.106.
18. S. Zhang et al.: Acta Biomaterialia, 6(2), 2010, 626-640. https://doi.org/10.1016/j.actbio.2009.06.028.
19. N. Ikeo, M. Nishioka, T. Mukai: Materials Letters, 223, 2018, 65-68. https://doi.org/10.1016/j.matlet.2018.03.188.
20. K. Wei Guo: Recent Patents on Corrosion Science, 1(1), 2011, 72-90.
21. Y. Sun, B. Zhang, Y. Wang, L. Geng , X. Jiao, Materials & Design, 34, 2012, 58-64. https://doi.org/10.1016/j.matdes.2011.07.058.
22. T. Li, H. Zhang, Y. He, N. Wen, X. Wang, Journal of Materials Science & Technology, 31(7), 2015, 744-750. https://doi.org/10.1016/j.jmst.2015.02.001.
23. H. Hornberger, S. Virtane, A. R. Boccaccini: Acta Biomaterialia, 8(7), 2012, 2442-2455. https://doi.org/10.1016/j.actbio.2012.04.012.
24. Y. Lu, A. R. Bradshaw, Y. L. Chiu, I. P. Jones: Materials Science and Engineering: C, 48, 2015, 480-486. https://doi.org/10.1016/j.msec.2014.12.049.
25. D. H. Cho, J. H. Nam, B. W. Lee, K. M. Cho, I. M. Park: Journal of Alloys and Compounds, 676, 2016, 461-468. https://doi.org/10.1016/j.jallcom.2016.03.182.
26. D. Dash, S. Samanta, R. N. Rai: IOP Conference Series: Materials Science and Engineering, 377, 2018, 012133. http://dx.doi.org/10.1088/1757-899X/377/1/012133.
27. J. E. Oghenevweta, V. S. Aigbodion, G. B. Nyior, F. Asuke: Journal of King Saud University - Engineering Sciences, 28(2), 2016, 222-229. https://doi.org/10.1016/j.jksues.2014.03.009.
28. J. Bienia, M. Walczak, B. Surowska, J. Sobczak: Journal of Optoelectronics and Advanced Materials, 5(2), 2003, 493-502.
29. M. P. Groover: *Fundamentals of modern manufacturing: materials, processes, and systems*. John Wiley & Sons, Inc., Hoboken, New Jersey, USA, 2020.
30. G. Parande, V. Manakari, S. D. Sharma Kopparthy, M. Gupta: Composites Part B: Engineering, 182, 2020, 107650. https://doi.org/10.1016/j.compositesb.2019.107650.
31. K. K. Deng, X. J. Wang, K. Wu: Materials Research Innovations, 18(sup4), 2014, S4-505-S504-509. https://doi.org/10.1179/1432891714Z.000000000728.
32. G. Parande, V. Manakari, S. D. S. Kopparthy, M. Gupta: Advanced Engineering Materials, 20(5), 2018, 1700919. https://doi.org/10.1002/adem.201700919.
33. K. S. Tun, P. Jayaramanavar, Q. B. Nguyen, J. Chan, R. Kwok, M. Gupta: Materials Science and Technology, 28(5), 2012, 582-588. https://doi.org/10.1179/1743284711Y.0000000108.
34. S. Seetharaman, J. Subramanian, K. S. Tun, A. S. Hamouda, M. Gupta: Materials, 6(5), 2013, 1940-1955. http://doi.org/10.3390/ma6051940.
35. D. J. Lloyd, International Materials Reviews, 39(1), 1994, 1-23. https://doi.org/10.1179/imr.1994.39.1.1.
36. G. E. Dieter, D. J. Bacon: *Mechanical metallurgy*. McGraw-Hill, New York, 1986.
37. *Standard practice for calculation of corrosion rates and related information from electrochemical measurements*, ASTM International, West Conshohocken, PA, 2015. http://doi.org/10.1520/G0102-89R15E01.
38. Z. Li, X. Gu, S. Lou, Y. Zheng: Biomaterials, 29(10), 2008, 1329-1344. https://doi.org/10.1016/j.biomaterials.2007.12.021.
39. H. R. Bakhsheshi-Rad et al.: Journal of Materials Engineering and Performance, 26(2), 2017, 653-666. https://doi.org/10.1007/s11665-016-2499-0.